

## Analysis of PUGNAc and NAG-thiazoline as Transition State Analogues for Human O-GlcNAcase: Mechanistic and Structural Insights into Inhibitor Selectivity and Transition State Poise

Garrett E. Whitworth,<sup>†</sup> Matthew S. Macauley,<sup>†</sup> Keith A. Stubbs,<sup>†</sup> Rebecca J. Dennis,<sup>‡</sup> Edward J. Taylor,<sup>‡</sup> Gideon J. Davies,<sup>‡</sup> Ian R. Greig,<sup>§</sup> and David J. Vocadlo<sup>\*,†</sup>

Contribution from the Department of Chemistry, Simon Fraser University, 8888 University Drive, Burnaby, British Columbia, Canada V5A 1S6, York Structural Biology Laboratory, Department of Chemistry, University of York, York YO10 5YW, U.K., and Department of Chemistry, University of Bath, Bath BA2 7AY, U.K.

E-mail: [dvocadlo@sfu.ca](mailto:dvocadlo@sfu.ca)

**Abstract:** O-GlcNAcase catalyzes the cleavage of  $\beta$ -O-linked 2-acetamido-2-deoxy- $\beta$ -D-glucopyranoside (O-GlcNAc) from serine and threonine residues of post-translationally modified proteins. Two potent inhibitors of this enzyme are O-(2-acetamido-2-deoxy-D-glucopyranosylidene)amino-N-phenylcarbamate (PUGNAc) and 1,2-dideoxy-2'-methyl- $\alpha$ -D-glucopyranosylidene- $\Delta$ 2'-thiazoline (NAG-thiazoline). Derivatives of these inhibitors differ in their selectivity for human O-GlcNAcase over the functionally related human lysosomal  $\beta$ -hexosaminidases, with PUGNAc derivatives showing modest selectivities and NAG-thiazoline derivatives showing high selectivities. The molecular basis for this difference in selectivities is addressed as is how well these inhibitors mimic the O-GlcNAcase-stabilized transition state (TS). Using a series of substrates, ground state (GS) inhibitors, and transition state mimics having analogous structural variations, we describe linear free energy relationships of  $\log(K_M/k_{cat})$  versus  $\log(K_I)$  for PUGNAc and NAG-thiazoline. These relationships suggest that PUGNAc is a poor transition state analogue, while NAG-thiazoline is revealed as a transition state mimic. Comparative X-ray crystallographic analyses of enzyme–inhibitor complexes reveal subtle molecular differences accounting for the differences in selectivities between these two inhibitors and illustrate key molecular interactions. Computational modeling of species along the reaction coordinate, as well as PUGNAc and NAG-thiazoline, provide insight into the features of NAG-thiazoline that resemble the transition state and reveal where PUGNAc fails to capture significant binding energy. These studies also point to late transition state poise for the O-GlcNAcase catalyzed reaction with significant nucleophilic participation and little involvement of the leaving group. The potency of NAG-thiazoline, its transition state mimicry, and its lack of traditional transition state-like design features suggest that potent rationally designed glycosidase inhibitors can be developed that exploit variation in transition state poise.

### Introduction

The development of rationally designed potent glycoside hydrolase inhibitors has been a topic of continuing research for years and has more recently enjoyed a surge of interest due to their increased uses as both research tools<sup>1,2</sup> and as therapeutic agents.<sup>3–5</sup> Considerable efforts have been directed toward preparing both potent<sup>6–8</sup> and selective<sup>9–11</sup> glycosidase inhibitors

using transition state (TS) mimicry as a guiding design principle.<sup>7,8</sup> The expectation that stable molecules resembling the enzyme catalyzed transition state, in either their charge or geometry, will be potent competitive inhibitors stems from a proposal, made first by Pauling,<sup>12</sup> that enzymes catalyze reactions by binding interactions realized preferentially with the transition state rather than with ground state (GS).<sup>12,13</sup> Such tight binding stabilizes these fleeting transition state structures and

<sup>†</sup> Simon Fraser University.

<sup>‡</sup> University of York.

<sup>§</sup> University of Bath.

- (1) Tulp, A.; Barnhoorn, M.; Bause, E.; Ploegh, H. *EMBO J.* **1986**, *5*, 1783–1790.
- (2) Vosseller, K.; Wells, L.; Lane, M. D.; Hart, G. W. *Proc. Natl. Acad. Sci. U.S.A.* **2002**, *99*, 5313–5318.
- (3) Butters, T. D.; Dwek, R. A.; Platt, F. M. *Adv. Exp. Med. Biol.* **2003**, *535*, 219–226.
- (4) von Itzstein, M.; et al. *Nature* **1993**, *363*, 418–423.
- (5) Mendel, D. B.; et al. *Antimicrob. Agents Chemother.* **1998**, *42*, 640–646.
- (6) Vasella, A.; Davies, G. J.; Bohm, M. *Curr. Opin. Chem. Biol.* **2002**, *6*, 619–629.

- (7) Stutz, A. E. *Iminosugars as Glycosidase Inhibitors, Nojirimycin and Beyond*; John Wiley and Sons: Weinheim, 1999.
- (8) Lillelund, V. H.; Jensen, H. H.; Liang, X.; Bols, M. *Chem. Rev.* **2002**, *102*, 515–553.
- (9) Macauley, M. S.; Whitworth, G. E.; Debowski, A. W.; Chin, D.; Vocadlo, D. J. *J. Biol. Chem.* **2005**, *280*, 25313–25322.
- (10) Siriwardena, A.; Strachan, H.; El-Daher, S.; Way, G.; Winchester, B.; Glushka, J.; Moremen, K.; Boons, G. J. *ChemBioChem* **2005**, *6*, 845–848.
- (11) Ho, C. W.; Lin, Y. N.; Chang, C. F.; Li, S. T.; Wu, Y. T.; Wu, C. Y.; Liu, S. W.; Li, Y. K.; Lin, C. H. *Biochemistry* **2006**, *45*, 5695–702.
- (12) Pauling, L. *Nature* **1948**, *161*, 707–709.
- (13) Jencks, W. P. K.; N. O.; Kennedy, E. P. *Academic* **1966**, 273–298.

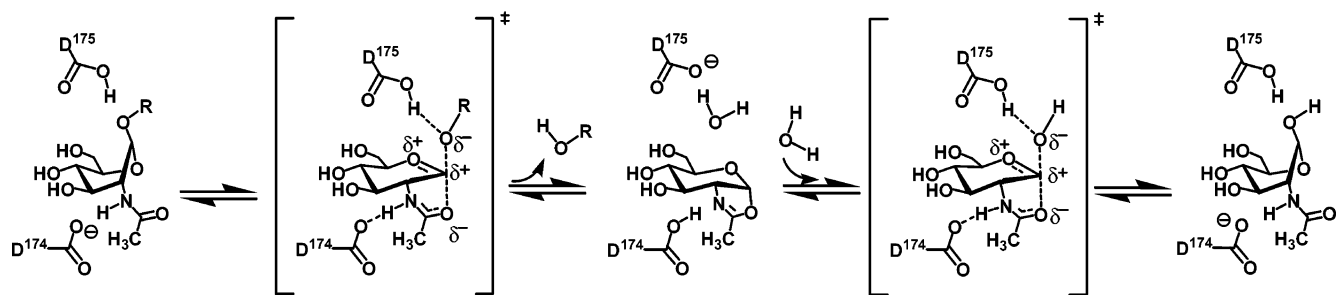


**Figure 1.** Catalytic mechanism used by *O*-GlcNAcase involves substrate-assisted catalysis. The first step of the reaction, cyclization, proceeds via attack of the 2-acetamido carbonyl oxygen on the anomeric center to form a covalent bicyclic oxazoline intermediate. This step is facilitated by polarization of the 2-acetamido moiety by an enzymic carboxyl group most likely acting as a general base catalyst. Departure of the aglycone is facilitated by general acid catalysis provided by another carboxyl group in the enzyme active site. In the second step, ring opening, the oxazoline intermediate is broken open by the general base-catalyzed attack of a water molecule on the anomeric center and general acid catalysis facilitating departure of the amide group. Both steps occur with inversion of stereochemistry at the anomeric center such that the overall reaction proceeds with net retention of stereochemistry.

thereby results in the enormous rate accelerations of up to  $10^{19}$ -fold seen for the most proficient enzymes.<sup>14</sup> On the basis of this rate acceleration the theoretical limit for the dissociation constant of a perfect transition state analogue can be estimated to be approximately  $10^{-22}$  M.<sup>14</sup> Of course, stable transition state analogues necessarily vary from genuine transition state structures having partial bonds, and therefore it is impossible to capture all the potentially available binding energy using a stable molecule. Despite this limitation, very potent transition state analogues have been found for several different classes of enzymes.<sup>15,16</sup>

For certain enzyme classes, extensive kinetic isotope effect studies have been carried out that have enabled the definition of geometric and electrostatic features of the transition state.<sup>17,18</sup> Such studies have led to the development of very tight binding inhibitors that are now clinical drug candidates.<sup>19</sup> For glycosidases, however, despite considerable synthetic efforts the very best inhibitors rationally designed as transition state analogues typically have no lower than nanomolar affinities.<sup>6–8</sup> Although highly detailed kinetic isotope effect studies of the glycoside hydrolases are lacking, a significant body of data has accrued that provides limited insights into the general features of transition states found for these enzymes.<sup>20,21</sup>

Large and normal secondary  $\alpha$ -D kinetic isotope effect studies suggest that these transition states have an  $sp^2$ -hybridized anomeric center with significant oxocarbenium ion-like character.<sup>21,22</sup> A corollary of such presumed planar oxocarbenium ion-like transition states is that the pyranose ring is expected to assume a conformation in which the C-2, C-1, C-5, and O-5 atoms adopt a coplanar arrangement.<sup>20</sup> Such limited kinetic isotope effects, in conjunction with Brønsted analyses using substrates having different leaving group abilities, have generally suggested transition states in which the leaving group is largely dissociated.<sup>21</sup> Accordingly, the vast majority of rationally designed glycosidase inhibitors exploit three principle design features.<sup>6–8</sup> First, an  $sp^2$ -hybridized center is often installed at

C-1 of the pyranose ring to mimic the geometric requirements of the putative planar oxocarbenium ion-like transition state. Second, nitrogen is often incorporated in place of C-1 or O-5 to mimic the relative positive charge development at these centers within the transition state. Third, and less commonly, conformationally constrained inhibitors are used that force the pyranose ring to adopt a transition state-like conformation.<sup>6,23–25</sup>

Many inhibitors are defined as transition state analogues by virtue of the principles used in their design and their superficial resemblance to predicted transition state structures. In only a very few cases have efforts been made to define whether these molecules are genuinely transition state analogues, simply serendipitous binders, or actually ground state analogues. Here we investigate the binding of two known potent inhibitors to human *O*-GlcNAcase; a family (for the classification of glycoside hydrolases see the CAZY database; <http://afmb.cnrs-mrs.fr/CAZY>) 84 glycoside hydrolase catalyzing the cleavage of *O*-linked 2-acetamido-2-deoxy- $\beta$ -D-glucopyranoside (*O*-GlcNAc) from serine and threonine residues of post-translationally modified nuclear and cytoplasmic proteins.<sup>26,27</sup> Our objective being to gain insight into the design of potent transition state analogues as well as to evaluate why *O*-(2-acetamido-2-deoxy-D-glucopyranosylidene)amino-*N*-phenylcarbamate (PUGNAc, Figure 2, **1a–g**) based derivatives bearing bulky *N*-acyl groups show weak selectivity<sup>28,29</sup> for human *O*-GlcNAcase over human lysosomal  $\beta$ -hexosaminidase, while analogous derivatives of 1,2-dideoxy-2'-methyl- $\alpha$ -D-glucopyranosyl-[2,1-*d*]- $\Delta$ 2'-thiazoline (NAG-thiazoline, Figure 2, **2a–g**) show high selectivities.<sup>9</sup>

*O*-GlcNAcase uses a two-step catalytic mechanism involving substrate-assisted catalysis<sup>9,30</sup> to form a transient oxazoline intermediate<sup>31</sup> (Figure 1) that is broken down to liberate the free sugar hemiacetal and the protein. This overall catalytic

(14) Wolfenden, R.; Snider, M. J. *Acc. Chem. Res.* **2001**, *34*, 938–945.  
 (15) Bartlett, P. A.; Marlowe, C. K. *Biochemistry* **1983**, *22*, 4618–4624.  
 (16) Lewandowicz, A.; Tyler, P. C.; Evans, G. B.; Furneaux, R. H.; Schramm, V. L. *J. Biol. Chem.* **2003**, *278*, 31465–31468.  
 (17) Schramm, V. L. *Acc. Chem. Res.* **2003**, *36*, 588–596.  
 (18) Berti, P. J.; Tanaka, K. S. E. *Adv. Phys. Org. Chem.* **2002**, *37*, 239–314.  
 (19) Gandhi, V.; Kilpatrick, J. M.; Plunkett, W.; Ayres, M.; Harman, L.; Du, M.; Bantia, S.; Davison, J.; Wierda, W. G.; Faderl, S.; Kantarjian, H.; Thomas, D. *Blood* **2005**, *106*, 4253–4260.  
 (20) Sinnott, M. L. *Chem. Rev.* **1990**, *90*, 1171–1202.  
 (21) Davies, G. J.; Sinnott, M. L.; Withers, S. G. *Comprehensive Biological Catalysis*; Sinnott, M. L., Ed.; 1998; Vol 1, pp 119–209.  
 (22) Sinnott, M. L.; Souchard, I. J. *Biochem. J.* **1973**, *133*, 89–98.

(23) Tanaka, K. S. E.; Winters, G. C.; Batchelor, R. J.; Einstein, F. W. B.; Bennet, A. J. *J. Am. Chem. Soc.* **2001**, *123*, 998–999.  
 (24) Mosi, R.; Sham, H.; Uitdehaag, J. C. M.; Ruiterkamp, R.; Dijkstra, B. W.; Withers, S. G. *Biochemistry* **1998**, *37*, 17192–17198.  
 (25) Berland, C. R.; Sigurskjold, B. W.; Stoffer, B.; Frandsen, T. P.; Svensson, B. *Biochemistry* **1995**, *34*, 10153–10161.  
 (26) Dong, D. L. Y.; Hart, G. W. *J. Biol. Chem.* **1994**, *269*, 19321–19330.  
 (27) Gao, Y.; Wells, L.; Comer, F. I.; Parker, G. J.; Hart, G. W. *J. Biol. Chem.* **2001**, *276*, 9838–45.  
 (28) Stubbs, K. A.; Zhang, N.; Vocadlo, D. J. *Org. Biomol. Chem.* **2006**, *4*, 839–845.  
 (29) Kim, E. J.; Perreira, M.; Thomas, C. J.; Hanover, J. A. *J. Am. Chem. Soc.* **2006**, *128*, 4234–4235.  
 (30) Cetinbas, N.; Macauley, M. S.; Stubbs, K. A.; Drapala, R.; Vocadlo, D. J. *Biochemistry* **2006**, *45*, 3835–3844.  
 (31) Macauley, M. S.; Stubbs, K. A.; Vocadlo, D. J. *J. Am. Chem. Soc.* **2005**, *127*, 17202–17203.

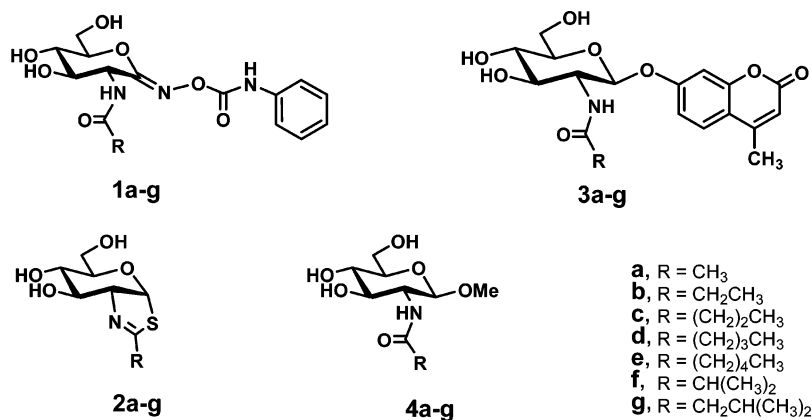


**Figure 2.** Series of inhibitors and substrates used to study transition state analogy of PUGNAc and NAG-thiazoline.

mechanism is common to glycosidases from families 18, 20, 56, and 84, all of which have evolved two strategically positioned carboxyl residues located within the active site that play key catalytic roles.<sup>32–35</sup> Asp<sup>174</sup> and Asp<sup>175</sup> have been identified as the two key catalytic residues of human *O*-GlcNAcase.<sup>30,36</sup> In the first step of the reaction, the cyclization step, Asp<sup>174</sup> directs and polarizes the 2-acetamido group to act as a nucleophile and form the oxazoline intermediate.<sup>30</sup> Asp<sup>175</sup> meanwhile acts as a general acid, encouraging departure of the aglycone leaving group.<sup>30</sup> In the second step, ring-opening, Asp<sup>174</sup> facilitates departure of the 2-acetamido group, while Asp<sup>175</sup> acts as a general base, promoting the attack of a molecule of water to yield the  $\beta$ -hemiacetal product.<sup>30</sup> The structure of the two transition states flanking the oxazoline intermediate have been investigated through substrate structure–function studies<sup>9,30</sup> and  $\alpha$ -D kinetic isotope effects.<sup>31</sup> These studies have suggested an “exploded” S<sub>N</sub>1-like transition state in which both the leaving group and nucleophilic carbonyl oxygen of the acetamido group are distant from the anomeric center. Similar proposals have been made for the mechanistically related family 20  $\beta$ -hexosaminidases.<sup>37</sup> The most common interpretation of the geometric and electrostatic structure of such transition states for enzymes using substrate-assisted catalysis is that the transition states are oxocarbenium ion-like with an sp<sup>2</sup>-hybridized anomeric center and delocalized positive charge between the endocyclic ring oxygen and the anomeric center.<sup>20–22</sup>

The two best characterized inhibitors of *O*-GlcNAcase are PUGNAc and NAG-thiazoline. PUGNAc, first prepared by Vasella and co-workers,<sup>38</sup> has been proposed to be a transition state analogue<sup>39</sup> by virtue of its sp<sup>2</sup>-hybridized anomeric center which is thought to have geometric resemblance to an oxocarbenium ion-like transition state (Figure 1). NAG-thiazoline, first prepared by Knapp and co-workers,<sup>40</sup> is a highly potent

competitive inhibitor of both the family 20  $\beta$ -hexosaminidases<sup>34,40</sup> and the family 84 *O*-GlcNAcases.<sup>9</sup> This molecule has an obvious geometric resemblance to the oxazoline intermediate, although it has been suggested it may bind tightly by virtue of its resemblance to a geometrically related transition state. Whether these two highly potent inhibitors of *O*-GlcNAcase are truly transition state analogues, however, has yet to be determined.

Using a combination of linear free energy analyses, computational modeling studies, and X-ray crystallographic analysis of enzyme–inhibitor complexes, we evaluate whether these two inhibitors bind as transition state analogues, ground state analogues, or serendipitous binders. New insights into the structure of the transition state for the *O*-GlcNAcase catalyzed hydrolysis of glycosides are gained and, by analogy, into those of related enzymes using such a substrate-assisted catalytic mechanism.

## Results and Discussion

The successful application of the principles of enzymology to the design of transition state analogues can be gauged by the increasing numbers of potent, rationally designed, transition state analogues. For many inhibitors few criteria, other than their potency, are used to define them as transition state analogues. In many cases, the designation of transition state analogue may be inadvertently misused to describe opportunistic inhibitors that simply exploit favorable binding situations within enzyme active sites. In recent years there has only been limited progress in developing still more potent transition state analogues of glycoside hydrolase inhibitors. Studies directed at clarifying which inhibitors are transition state analogues, however, have proven value in improving our understanding of transition state structures as well as in the iterative design of improved transition state analogues. We therefore have undertaken studies to define the mode of binding of two well-characterized inhibitors of human *O*-GlcNAcase: NAG-thiazoline and PUGNAc.

Both NAG-thiazoline and PUGNAc are potent inhibitors of *O*-GlcNAcase (Table 1) and bind nearly 240 000-fold more tightly than the ground state inhibitor methyl 2-acetamido-2-deoxy- $\beta$ -D-glucopyranoside **4a** ( $K_1 = 11$  mM, Table 1). Potent inhibition alone, however, is not a good measure of transition state analogy, and several other more rigorous approaches have been advanced.<sup>15,41–44</sup> Arguably, the most rigorous approach to establishing transition state analogy has been to use free energy correlations between inhibitor binding and transition state

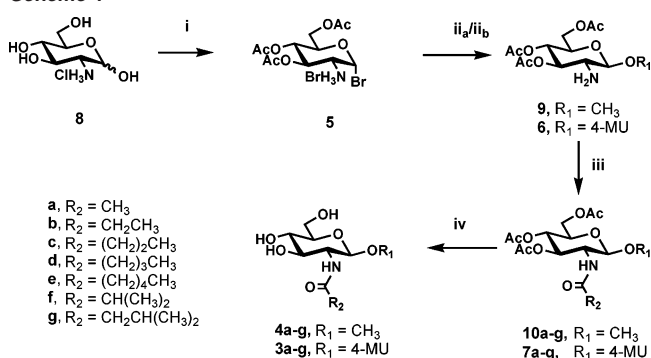
- (32) van Aalten, D. M.; Komander, D.; Synstad, B.; Gaseidnes, S.; Peter, M. G.; Eijlsink, V. G. *Proc. Natl. Acad. Sci. U.S.A.* **2001**, *98*, 8979–8984.
- (33) Tewes, I.; Perrakis, A.; Oppenheim, A.; Dauter, Z.; Wilson, K. S.; Vorgias, C. E. *Nat. Struct. Biol.* **1996**, *3*, 638–648.
- (34) Mark, B. L.; Vocadlo, D. J.; Knapp, S.; Triggs-Raine, B. L.; Withers, S. G.; James, M. N. J. *Biol. Chem.* **2001**, *276*, 10330–10337.
- (35) Markovic-Housley, Z.; Miglierini, G.; Soldatova, L.; Rizkallah, P. J.; Muller, U.; Schirmer, T. *Structure* **2000**, *8*, 1025–1035.
- (36) Toleman, C.; Paterson, A. J.; Kudlow, J. E. *Biochim. Biophys. Acta* **2006**, *1760*, 829–839.
- (37) Vocadlo, D. J.; Withers, S. G. *Biochemistry* **2005**, *44*, 12809–12818.
- (38) Beer, D.; Maloisel, J. L.; Rast, D. M.; Vasella, A. *Helv. Chim. Acta* **1990**, *73*, 1918–1922.
- (39) Rao, F. V.; Dorfmueller, H. C.; Villa, F.; Allwood, M.; Eggleston, I. M.; van Aalten, D. M. *EMBO J.* **2006**, *25*, 1569–1578.
- (40) Knapp, S.; Vocadlo, D.; Gao, Z. N.; Kirk, B.; Lou, J. P.; Withers, S. G. *J. Am. Chem. Soc.* **1996**, *118*, 6804–6805.

**Table 1.** Kinetic Data Determined Using Human *O*-GlcNAcase for the Three Series of Inhibitors and the Series of Substrates

R group	PUGNR		GlcNR-THZ		GlcNR <i>O</i> -Me	MU-Glc NR
	$K_I$ ( $\mu$ M)	selectivity (family (20/84))	$K_I$ ( $\mu$ M)	selectivity (family (20/84))	$K_{I(GS)}$ (mM)	$K_M/k_{cat}$ (mM min)
-CH <sub>3</sub>	0.046	1	0.07	1	11	0.13
-CH <sub>2</sub> CH <sub>3</sub>	1.2	1	0.12	270	11	0.15
-(CH <sub>2</sub> ) <sub>2</sub> CH <sub>3</sub>	2.5	11	0.25	1500	21	0.19
-(CH <sub>2</sub> ) <sub>3</sub> CH <sub>3</sub>	40	6	1.5	3100	70	1.8
-(CH <sub>2</sub> ) <sub>4</sub> CH <sub>3</sub>	220	≥5	57	100	205	1.8
-CH(CH <sub>3</sub> ) <sub>2</sub>	9	2	1.6	700	147	5.0
-CH <sub>2</sub> CH(CH <sub>3</sub> ) <sub>2</sub>	190	≥6	5.7	190	224	110

stabilization.<sup>15,44</sup> Using this method to distinguish whether an inhibitor is a transition state analogue, ground state analogue, or simply a fortuitous binder involves systematic modification of the inhibitor at one position and determining the resulting changes in  $K_I$  values. Analogous structural changes are also made within the substrate, and  $k_{cat}/K_M$  values are determined, since this parameter informs on the structure of the first transition state reached along the reaction coordinate. The inverse logarithm of these values provides free energy terms that, when correlated to each other in a plot of  $\log K_I$  versus  $\log K_M/k_{cat}$ , may yield one of several patterns.<sup>15,44,45</sup> The proper interpretation of these linear free energy diagrams rests on several practical assumptions:<sup>44</sup> (1) the chemical step having the transition state mimicked by the inhibitors must be rate limiting for the reaction, (2) the intrinsic reactivity of the substrates must not significantly change as a result of the modifications, and (3) variation of the substituent should not affect binding to the enzyme of the unmodified regions of either the substrate or inhibitor. Once these requirements are satisfied a strong correlation with a slope of 1 reveals the inhibitor is a transition state analogue. This interpretation stems from the expectation that changes made to a bona fide transition state analogue should evoke equivalent changes in the energy of the actual transition state when introduced within the substrate.<sup>46,47</sup> Conversely, scattered plots having weak correlations suggest the inhibitor is a poor transition state analogue or a fortuitous binding inhibitor.<sup>7</sup> Ground state mimics, on the other hand, are best revealed by strong correlations having a slope of 1 between  $\log K_I$  of the inhibitor and  $\log K_S$  values for binding of the substrate ( $\log K_I$  for a ground state analogue or  $\log K_M$  for enzymes with a rapid equilibrium substrate binding step may also be used).

It is noteworthy that in two closely related glycosidases from family 13, correlations of  $\log K_I$  versus  $\log K_M/k_{cat}$  have yielded slopes other than 1 and these have been interpreted in entirely different ways.<sup>24,25</sup> These two studies, however, have been carried out using enzymes in which mutations have been made at several different residues within their active sites. It therefore seems prudent to make systematic structural variations at only one site. The best approach, first described by the Bartlett group,<sup>15</sup> is to make a series of *small* structural perturbations to the inhibitor at *one* site since these are most likely to report in a sensitive manner on changes in the differences between the actual transition state and the putative transition state mimic.

**Scheme 1<sup>a</sup>**

<sup>a</sup> (i) AcBr, heat; (ii<sub>a</sub>) pyridine, MeOH; (ii<sub>b</sub>) (a) acetone, 4-MU, Na 4-MU; (b) K<sub>2</sub>CO<sub>3</sub>, Et<sub>2</sub>O; (c) HCl; (iii) RCOCl, Et<sub>3</sub>N, DCM; (iv) (a) NaOMe, MeOH; (b) 20:1 MeOH:acetic acid.

For *O*-GlcNAcases, we know that the *N*-acyl group of the substrate is critically involved in catalysis and must undergo conformational, electrostatic, and positional variation within the active site of the enzyme on proceeding from the ground state to the transition state.<sup>9,31</sup> We speculated that modifications of this group would report clearly on the transition state structure for these enzymes and that derivatives of PUGNAc (1) and NAG-thiazoline (2), both previously synthesized within our laboratory, would be useful probes.<sup>9,28</sup> The structural changes within these inhibitors are small increases in the volume of the alkyl group of the *N*-acyl moiety and they give rise to  $K_I$  values varying by over five orders of magnitude when assayed against human *O*-GlcNAcase (Table 1).<sup>28</sup> Such a wide variation in  $K_I$  values is beneficial for establishing a meaningful correlation. With these molecules already in hand, we then prepared (Scheme 1) the requisite series of substrates with analogous modifications to the *N*-acyl group and measured the second-order rate constants for human *O*-GlcNAcase catalyzed hydrolysis of these compounds (Table 1). Satisfying the first requirement of the transition state analogy approach (vide supra), we have previously shown, using a combination of kinetic isotope effects<sup>31</sup> and a series of substrates bearing different leaving groups,<sup>9,30</sup> that the second-order rate constant for substrates bearing the 4-methylumbelliferyl leaving group reflects the first chemical step. The second requirement of this approach is fulfilled since the spontaneous hydrolysis rates of these substrates are indistinguishable within error. Due to limitations in the solubility of these substrates, however, we were unable to obtain reliable  $K_S$  or even  $K_M$  values making correlations with  $K_S$  or  $K_M$  values impossible. A series of methyl glycosides (Figure 2, 4a-g) was therefore also prepared (Scheme 1) as simple ground state substrates and were tested as competitive inhibitors to obtain inhibition constants (Table 1) that are taken to be equivalent to true dissociation constants.

(41) Rahil, J.; Pratt, R. F. *Biochemistry* **1994**, *33*, 116–125.

(42) Dale, M. P.; Ensley, H. E.; Kern, K.; Sastry, K. A.; Byers, L. D. *Biochemistry* **1985**, *24*, 3530–3539.

(43) Snider, M. J.; Wolfenden, R. *Biochemistry* **2001**, *40*, 11364–11371.

(44) Mader, M. M.; Bartlett, P. A. *Chem. Rev.* **1997**, *97*, 1281–1301.

(45) Bartlett, P. A.; Giangordano, M. A. *J. Org. Chem.* **1996**, *61*, 3433–3438.

(46) Wolfenden, R. *Nature* **1969**, *223*, 704–705.

(47) Lienhard, G. E. *Science* **1973**, *180*, 149–154.



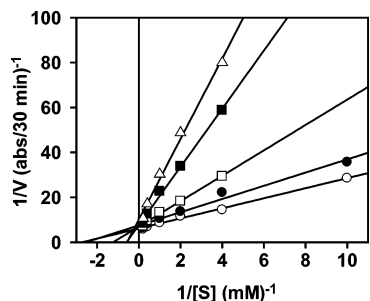


**Figure 3.** Inhibition of human *O*-GlcNAcase using ground state substrate methyl 2-acetamido-2-deoxy- $\beta$ -glucopyranoside. Inhibition of *O*-GlcNAcase catalyzed hydrolysis of *p*NP-GlcNAc by the methyl glycoside (**4a**) shows a pattern of competitive inhibition. The concentrations of **4a** (mM) used were 85.0 ( $\Delta$ ), 42.5 ( $\blacksquare$ ), 11.0 ( $\square$ ), 5.5 ( $\bullet$ ), and 0.0 ( $\circ$ ).

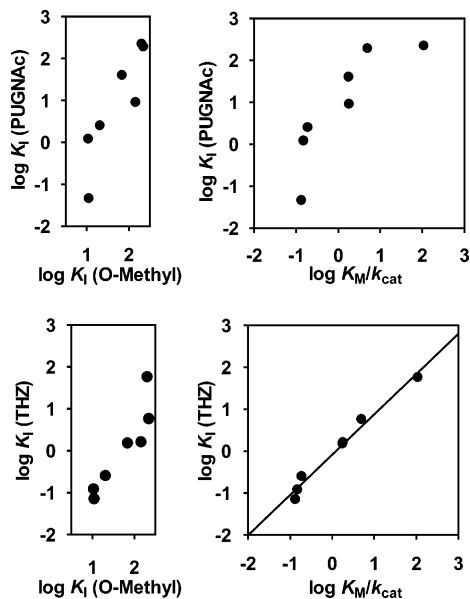


**Figure 4.** Comparison of transition state analogy free energy diagrams for NAG-thiazoline and PUGNAc derivatives. (A, top left) Comparison of PUGNAc series of inhibitors (**1a–g**)  $K_I$  with methyl glycoside series (**4a–g**)  $K_I$ . (B, top right) Comparison of PUGNAc series of inhibitors (**1a–g**)  $K_I$  with substrate (**3a–g**)  $K_M/k_{cat}$ . (C, bottom left) Comparison of thiazoline series of inhibitors (**2a–g**)  $K_I$  with methyl glycoside series (**4a–g**)  $K_I$ . (D, bottom right) Comparison of thiazoline series of inhibitors (**2a–g**)  $K_I$  with substrate (**3a–g**)  $K_M/k_{cat}$ .

Testing parent glycoside **4** as a representative member of these ground state inhibitors revealed, as expected, a pattern of competitive inhibition (Figure 3) and validated their use as ground state analogues binding within the *O*-GlcNAcase active site. Together, these four sets of compounds allowed us to delineate the nature of the inhibition of human *O*-GlcNAcase by NAG-thiazoline and PUGNAc.

Correlations of  $\log K_I$  values for the series of NAG-thiazoline derivatives (Figure 2, **2a–g**) with the corresponding logarithm of the inverse second-order rate constants  $K_M/k_{cat}$  for the *O*-GlcNAcase catalyzed hydrolysis of a series of 4-methylumbelliferyl glycoside substrates (Figure 2, **3a–g**) reveals a strong correlation ( $r^2 = 0.98$ ) with a slope of  $0.97 \pm 0.06$  (Figure 4D). This correlation indicates that the incremental differences in binding energy related to the elaboration of the thiazoline ring with aliphatic chains of increasing length are nearly identical to those perturbations observed for the transition state of the enzyme catalyzed hydrolysis of the substrates bearing analogous changes. Correlations of  $\log K_I$  values with the corresponding

logarithm of the inhibition constants ( $\log K_{I(GS)}$ ) for the ground state inhibitors showed no clear correlation (Figure 4C). These two patterns are very similar to those observed by Bartlett and co-workers,<sup>15,48</sup> which they used to show that phosphoramidates are transition state analogues for the zinc peptidases. Together these data strongly support the proposed mechanism involving substrate-assisted catalysis from the acetamido group and reveal NAG-thiazoline as a good transition state mimic for *O*-GlcNAcase catalyzed glycoside hydrolysis.

Using this approach, it is possible only to comment on the transition state resemblance in regions where the inhibitor varies in structure from the substrate. The specific structural features probed by NAG-thiazoline encompass the entire thiazoline ring, including the position of all associated atoms including C-1 and C-2 of the pyranose ring. Notably, C-1 of NAG-thiazoline is an  $sp^3$ -hybridized carbon center rather than an  $sp^2$ -hybridized center or basic nitrogen, features that are often assumed to be essential features of transition state mimics for glycoside hydrolases. The two best studied iminosugar inhibitors are the isofagomine class, wherein C-1 is replaced with nitrogen and the endocyclic ring oxygen with a methylene unit, and the nojirimycin class of inhibitors, wherein the endocyclic ring oxygen is replaced by a nitrogen atom. Both of these inhibitors have been proposed to be transition state mimics although more recent experimental data suggest that, at least for some enzymes, this is not the case. Indeed, in a crystallographic complex of GalNAc-isofagomine bound to a family 20  $\beta$ -hexosaminidase that uses substrate-assisted catalysis, it was observed that the protonated nitrogen engaged in an adventitious electrostatic interaction with the general acid/base catalytic residue.<sup>49</sup> For nojirimycin, scattered linear free energy data was observed for two related  $\alpha$ -glucosidases, suggesting that this inhibitor is an adventitious binder to the two enzymes studied.<sup>7,25</sup>

For the series of PUGNAc derivatives a poor correlation ( $r^2 = 0.73$ , Figure 4B) with a slope of  $1.07 \pm 0.29$  was observed in a plot of  $\log K_I$  values of the inhibitor versus  $\log K_M/k_{cat}$  values for the series of glycoside substrates. As well, a poor correlation is observed between  $\log K_I$  values and  $\log K_{I(GS)}$  values for the ground state inhibitors (Figure 4A). Accordingly, the scatter within both of these correlations indicates that incremental changes of the *N*-acyl chain of the parent compound are not viewed in a similar manner within the active site of the enzyme as the incremental elongation of the *N*-acyl chain of the substrate, indicating that PUGNAc is either a poor mimic of the *O*-GlcNAcase-catalyzed transition state or simply a fortuitous binder. Consistent with this interpretation, Bartlett has described scatter of the data as an indication that the inhibitor may not closely resemble the transition state.<sup>44</sup>

In the context of the traditional design principles used in developing transition state analogue inhibitors of glycosidases, the apparent weak transition state analogy of PUGNAc is surprising. The trigonal anomeric center found within PUGNAc is often considered to be a vitally important feature, and many potent inhibitors contain such a moiety. It is worth noting that NAG-thiazoline, which lacks all of the key design features of transition state analogues, is an equally potent inhibitor as PUGNAc. NAG-thiazoline may therefore mimic a transition

(48) Phillips, M. A.; Kaplan, A. P.; Rutter, W. J.; Bartlett, P. A. *Biochemistry* **1992**, *31*, 959–963.

(49) Mark, B. L.; Vocadlo, D. J.; Zhao, D.; Knapp, S.; Withers, S. G.; James, M. N. *J Biol. Chem.* **2001**, *276*, 42131–42137.

state that is significantly different than the canonical oxocarbenium ion-like transition state that is widely perceived to be found along the reaction coordinate of glycoside hydrolases.

In view of this possibility we considered previous results in this new context. The large secondary  $\alpha$ -deuterium kinetic isotope effects ( $\alpha$ D-KIE) of  $1.14 \pm 0.02$  measured previously<sup>31</sup> with human *O*-GlcNAcase suggests that the enzyme stabilized transition states have oxocarbenium ion-like character with significant  $sp^2$ -character at the anomeric center. Interpreting this KIE as revealing a strict trigonal geometry at the anomeric center in the transition state is complicated, however, as underscored by studies of known  $S_N2$  reactions of the methoxymethyl model system. Depending on the nature of the incoming nucleophile,  $\alpha$ D-KIE values traditionally held to be consistent with either  $S_N1$  ( $k_H/k_D = 1.18$ ) or  $S_N2$  ( $k_H/k_D = 0.99$ ) were observed.<sup>50</sup> Further complicating matters is that equilibrium isotope binding effects have been observed in several cases where deuterium is present at the anomeric center.<sup>51</sup> Accordingly, in the absence of other supporting heavy atom isotope effects at the reaction center, interpreting the magnitude of  $\alpha$ D-KIE values at acetal centers is difficult and cannot be used to discern the extent of nucleophilic participation.<sup>52</sup> Therefore, it seems equally possible that the  $\alpha$ D-KIE values determined may reflect a non-planar transition state having greater nucleophilic participation and correspondingly less p-orbital character at the anomeric center.

Such differences in the extent of nucleophilic participation and involvement of the leaving group have been well-documented for the *N*-ribosyl hydrolases and have developed with the support of X-ray crystallographic analyses of enzyme–inhibitor complexes into the concept of transition state poise. The transition state poise is defined by the bond orders between the anomeric center and both the leaving group and nucleophile, which can vary significantly as a function of the position of C-1 along the reaction coordinate. In this context the glycoside hydrolases,<sup>53</sup> like the *N*-ribosyl hydrolases, appear to use an electrophilic migration mechanism<sup>54</sup> for which the reaction coordinate diagram can be defined by the motion of the anomeric carbon and where the total bond order between the anomeric center, nucleophile, and leaving group is significantly less than 1. Within crystallographically visualized Michaelis complexes of  $\beta$ -D-glycoside hydrolases<sup>33,55</sup> the anomeric carbon typically adopts a position *above* the plane of the pyranose ring with the exocyclic oxygen hydrogen bonding to the general acid catalytic group. Within the newly formed intermediate, the anomeric carbon is now positioned *below* the plane of the pyranose ring bonded to the nucleophile. For *O*-GlcNAcase, this nucleophile is the carbonyl oxygen of the acetamido group. The transition state must accordingly resemble a structure sitting somewhere along this pathway defined by these two end points and not necessarily, as widely believed, equidistant between them as would be found for an oxocarbenium ion.

Taft-like linear free energy analyses ( $\log k_{cat}/K_M$  versus  $\sigma^*$ ) of the *O*-GlcNAcase catalyzed hydrolysis of *N*-fluoroacetamido glycosides have strongly implicated the acetamido group in nucleophilic participation at the transition state of the rate determining chemical step.<sup>9,31</sup> Furthermore, the linear free energy analyses we describe here indicate that NAG-thiazoline is a transition state analogue, an observation also consistent with nucleophilic participation since the anomeric carbon and the thiazoline sulfur atom are only 1.85 Å apart from each other. However, whether NAG-thiazoline geometrically resembles the transition state along the reaction coordinate, some point along the reaction coordinate that is close to this saddle, or that the enzyme catalyzed reaction is  $D_N + A_N$  with a short-lived, yet discrete oxocarbenium ion, as has been suggested for  $\beta$ -galactosidase by Richard and co-workers,<sup>56</sup> currently remains untested in any glycoside hydrolase.

Assuming the transition state resembles NAG-thiazoline, as suggested by the free energy analyses, one can approximate the bond orders to both the leaving group and nucleophile. By assuming the interatomic distance between C-1 and the carbonyl oxygen in the transition state is 1.85 Å (the length of the C–S bond length within NAG-thiazoline), a Pauling bond order of 0.26 to the nucleophile can be calculated. The Brønsted analyses and the  $\alpha$ D-KIE values previously measured for human *O*-GlcNAcase suggest little involvement of the leaving group in the transition state. On these bases and the crystallographic analyses of the *Bacteroides thetaiotaomicron* *O*-GlcNAcase homologue in complex with NAG-thiazoline, we estimate the bond order to the leaving group is nearly 0 (0.01). In this structure, a molecule of water sits approximately 2.8 Å above the anomeric carbon in a position that is expected to be occupied by the glycosidic oxygen of the substrate within the Michaelis complex, and it is held in position by a hydrogen bond to the enzymic general base catalyst.<sup>57</sup> These data, in combination with other studies of the glycosidase mechanism, suggest that human *O*-GlcNAcase possesses an oxocarbenium ion-like transition state which is significantly stabilized by nucleophilic participation of the 2-acetamido group. This nucleophilic participation, in combination with the action of the catalytic residue hydrogen bonding with the amide nitrogen (Asp<sup>174</sup> in human *O*-GlcNAcase and Asp<sup>242</sup> in the *B. thetaiotaomicron*  $\beta$ -glucosaminidase), delocalizes excess positive charge away from the C-1–O-5 region of the pyranose and on into the oxazoline ring. Such a dissociative transition state is consistent with the previously described Taft analyses,<sup>9,57</sup> kinetic isotope effects,<sup>31</sup> and the free energy analyses we detail here. It is also reminiscent of those determined empirically for *N*-ribosyl transferases using a  $D_N A_N$  mechanism but most likely involving slightly greater nucleophilic participation.<sup>17,58</sup>

To gain greater insight into the basis by which NAG-thiazoline mimics the transition state whereas PUGNAc does not, we carried out crystallographic analyses of the selective *O*-GlcNAcase inhibitor, NButGT, complexed to a bacterial homologue of human *O*-GlcNAcase. This *B. thetaiotaomicron*  $\beta$ -glucosaminidase is an excellent model of human

(50) Knier, B. L.; Jencks, W. P. *J. Am. Chem. Soc.* **1980**, *102*, 6789–6798.  
(51) Lewis, B. E.; Schramm, V. L. *J. Am. Chem. Soc.* **2003**, *125*, 4785–4798.  
(52) Huang, X. C.; Tanaka, K. S. E.; Bennet, A. J. *J. Am. Chem. Soc.* **1997**, *119*, 11147–11154.  
(53) Vocadlo, D. J.; Davies, G. J.; Laine, R.; Withers, S. G. *Nature* **2001**, *412*, 835–838.  
(54) Fedorov, A.; Shi, W.; Kicska, G.; Fedorov, E.; Tyler, P. C.; Furneaux, R. H.; Hanson, J. C.; Gainsford, G. J.; Larese, J. Z.; Schramm, V. L.; Almo, S. C. *Biochemistry* **2001**, *40*, 853–860.  
(55) Sulzenbacher, G.; Driguez, H.; Henrissat, B.; Schulein, M.; Davies, G. J. *Biochemistry* **1996**, *35*, 15280–15287.

(56) Richard, J. P.; Huber, R. E.; Heo, C.; Amyes, T. L.; Lin, S. *Biochemistry* **1996**, *35*, 12387–12401.  
(57) Dennis, R. J.; Taylor, E. J.; Macauley, M. S.; Stubbs, K. A.; Turkenburg, J. P.; Hart, S. J.; Black, G. N.; Vocadlo, D. J.; Davies, G. J. *Nat. Struct. Mol. Biol.* **2006**, *13*, 365–371.  
(58) Scheuring, J.; Berti, P. J.; Schramm, V. L. *Biochemistry* **1998**, *37*, 2748–2758.

**Table 2.** Data Collection and Refinement Statistics for the Structure Solution of *B. thetaiotaomicron* GH84 *O*-GlcNAcase with NButGT

		<i>Bt</i> GH84 with <i>N</i> -butylthiazoline
Data Collection		
space group		<i>C</i> 2
cell dimens		
<i>a</i> , <i>b</i> , <i>c</i> (Å)		185.1, 51.7, 172.8
$\alpha$ , $\beta$ , $\gamma$ (deg)		90.0, 100.1, 90.0
wavelength		0.9930
resolution (Å)		40–2.25 (2.33–2.25) <sup>a</sup>
<i>R</i> <sub>sym</sub> or <i>R</i> <sub>merge</sub>		0.086 (0.47)
<i>I</i> / $\sigma$ ( <i>I</i> )		18 (3)
completeness (%)		99.9 (99.9)
redundancy		4.5 (4.4)
Refinement		
resolution (Å)		2.25
no. of reflcns		77 267
<i>R</i> <sub>work</sub> / <i>R</i> <sub>free</sub>		21/28
no. of atoms		
protein		9500
ligand		32
waters		554
<i>B</i> -factors		
protein		30
ligand/ion		19
water		30
RMS deviations		
bond lengths (Å)		0.023
bond angles (deg)		1.99

<sup>a</sup> Highest-resolution shell is shown in parentheses.

*O*-GlcNAcase since it too processes *O*-GlcNAc modified proteins and also has striking sequence conservation when compared to the human *O*-GlcNAcase. The structure of the *B. thetaiotaomicron* GH84 *O*-GlcNAcase, in complex with NButGT was solved at a resolution of 2.25 Å by molecular replacement (Table 2). The structure crystallized in a *C*2 space group (see methods) in which two molecules of *Bt*GH84 lie in the asymmetric unit in the same orientation separated by a translation-only vector of 0, 0, 0.5. The *Bt*GH84 structure can be traced from residue 4 of the mature protein through to residue 589, with two short breaks in molecule B from 51 to 53 and from 455 to 456. The C-terminal “CBM32-like”  $\beta$ -sheet domain, which was partially ordered in the original native structure solution, is completely disordered in this crystal form and could not be modeled. We compared the structure of this complex with a previously determined structure of NAG-thiazoline bound to the same enzyme<sup>57</sup> as well as to a complex of PUGNAc bound within the active site of a *Clostridium perfringens* homologue<sup>39,59</sup> of *O*-GlcNAcase. Gratifyingly, NButGT and NAG-thiazoline bind identically within the active site, and the pyranose ring of the inhibitors within both complexes can be overlaid exactly (data not shown). We find the only difference between the two structures is where electron density corresponding to the alkyl chain of NButGT extends into an active site pocket (Figure 5A) that has been previously predicted to accommodate such bulkier groups.<sup>9,57</sup> The confirmation of identical binding modes for the parent inhibitor and NButGT is important in the context of the transition state analogy studies described here since it satisfies the third implicit assumption of the approach that analogous inhibitors bind in the same orientation.

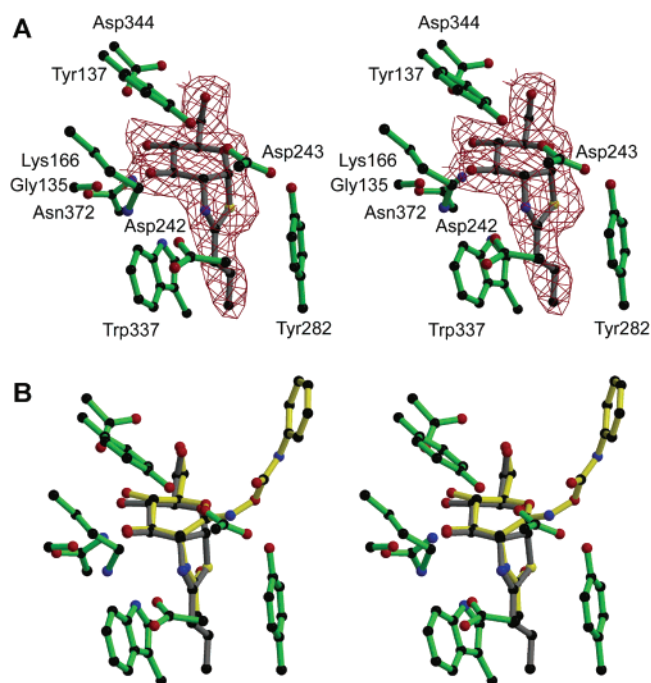


**Figure 5.** Structural analyses of the binding of NButGT to *Bt*GH84 and its comparison to binding of PUGNAc to *Cf*GH84. (A) Observed electron density for the NButGT along with its flanking residues. The map shown is a  $2F_{\text{obs}} - F_{\text{calc}}$  electron density map contoured at  $1\sigma$  and is shown in divergent (“walled”) stereo. (B) Structural overlap of the *Bt*GH84 NButGT complex (ligand, gray; protein, green) with the PUGNAc complex of the *Clostridium perfringens* GH84 enzyme<sup>39</sup> (yellow). The overlap was optimized using the main-chain protein atoms only, in a radius of 15 Å of the ligands, using the program QUANTA (Accelrys, San Diego, CA). This figure was drawn using MOLSCRIPT<sup>63</sup> and BOBSCRIPT.<sup>64</sup>

It has been noted previously by us that derivatives of PUGNAc having bulky *N*-acyl groups show weak selectivity toward human *O*-GlcNAcase over human  $\beta$ -hexosaminidase,<sup>28,29</sup> while the analogous NAG-thiazoline derivatives show high selectivities.<sup>9</sup> In an effort to better understand the molecular basis for these differences in selectivity, we decided to compare the binding modes of NButGT and PUGNAc by overlaying the structures of these two inhibitors bound to the *O*-GlcNAcase homologues (Figure 5B). The molecular basis for this discrepancy in selectivity must stem from structural differences between these molecules and how they interact with the active site of human *O*-GlcNAcase.

There are several obvious structural differences between NAG-thiazoline and PUGNAc. The first, and most obvious difference is that PUGNAc bears a phenyl carbamate moiety which is absent in NAG-thiazoline. This substituent extends out from the active site and engages in several interactions that are not found for NAG-thiazoline. The exocyclic oxime nitrogen of PUGNAc hydrogen bonds with the general acid/base catalytic group (Asp<sup>175</sup> within human *O*-GlcNAcase<sup>30</sup> and Asp<sup>243</sup> within the *B. thetaiotaomicron*  $\beta$ -glucosaminidase<sup>57</sup>), and the phenyl group of PUGNAc also engages in several hydrophobic and stacking interactions with residues in the aglycon binding site. It is interesting to note that *N*-acetylglucosamino-1,5-lactone oxime (LOGNAc), which lacks the phenyl carbamate group of PUGNAc, binds 30-fold more poorly<sup>26</sup> than PUGNAc, providing an indication of the importance of these serendipitous interactions. A second structural difference between the two inhibitors is that the hybridization at the anomeric center varies. This

(59) Ficko-Blean, E.; Boraston, A. B. *Acta Crystallogr., Sect. F: Struct. Biol. Cryst. Commun.* **2005**, *61*, 834–836.



variation has an impact on the preferred conformation of the pyranose ring; for PUGNAc the pyranose ring adopts a  ${}^4E$  conformation enforced, in part, by the  $sp^2$ -hybridized anomeric center, whereas NButGT sits in a  ${}^4C_1$  chair that is slightly distorted toward the  ${}^4E$  conformation due to the rigidity of the thiazoline ring. The structural consequence of these variations is that the substituents of the pyranose ring, particularly the 3- and 4-hydroxyl groups, adopt subtly different orientations. Such apparently minor differences in the position of both ring and substituent atoms can have pronounced effects on both van der Waals interactions and hydrogen bonds. A third obvious structural difference is that the *N*-acyl group of PUGNAc is free, while NAG-thiazoline's orientation is locked. This difference also results in important variations in the  $pK_a$  of the protonated nitrogen at the 2-position of the pyranose ring that will be discussed in greater detail in context of the computational studies (vide infra). The thiazoline ring is nestled between two tryptophan residues which presumably serve to accurately position the acetamido group of the substrate and stabilize the positive charge that develops at the transition state during formation of the oxazoline ring. Not only does the thiazoline ring engage in stacking interactions with these residues, but it also orients the alkyl substituent of the inhibitors. As seen in the structural comparison, (Figure 5), the alkyl substituent of NButGT is pointing directly down the active site cavity, whereas the *N*-acetamido group of PUGNAc is pointed at a slightly different angle. Consistent with this structural view, human *O*-GlcNAcase is better able to cope with elongation of the aliphatic chain of NAG-thiazoline derivatives as compared to analogous derivatives of PUGNAc (Table 1). Because van der Waals forces are powerfully distance-dependent, this apparently small difference may account for the significant differences in selectivity observed by us between the derivatives of these two families of inhibitors.

These crystallographic analyses primarily furnish details of the geometric features mediating interactions in the enzyme–inhibitor complexes but do not provide great insight into transition state structure nor the electrostatic features of the inhibitors and reaction coordinate species. We therefore reasoned that further insight into the potency, transition state analogy, and selectivity of both NAG-thiazoline- and PUGNAc-derived compounds toward human *O*-GlcNAcase could be gained from a comparison of their molecular electrostatic potential surfaces (MEPs) with that of the enzyme-bound intermediate or, better still, the enzymic transition state. Work by the Schramm group has shown that the similarity of transition states and inhibitors may be probed qualitatively and quantitatively using MEPs.<sup>60</sup> Accordingly, we modeled both inhibitors, PUGNAc-analogue **I** and NAG-Thiazoline **II**, as well as three species found along the reaction coordinate for the cyclization step (Figure 6C, bottom structures in color): an intact methyl glycoside ground state **III**, the transition state **IV** we predict on the basis of the TS analogy studies featuring a distorted oxazoline in which the C-1 carbonyl oxygen bond distance was constrained to the C-S bond distance within NAG-thiazoline,<sup>61</sup> and last the oxazoline intermediate **V** (Figure 6C, bottom structures in color). It is important to note that these species are expected to provide a

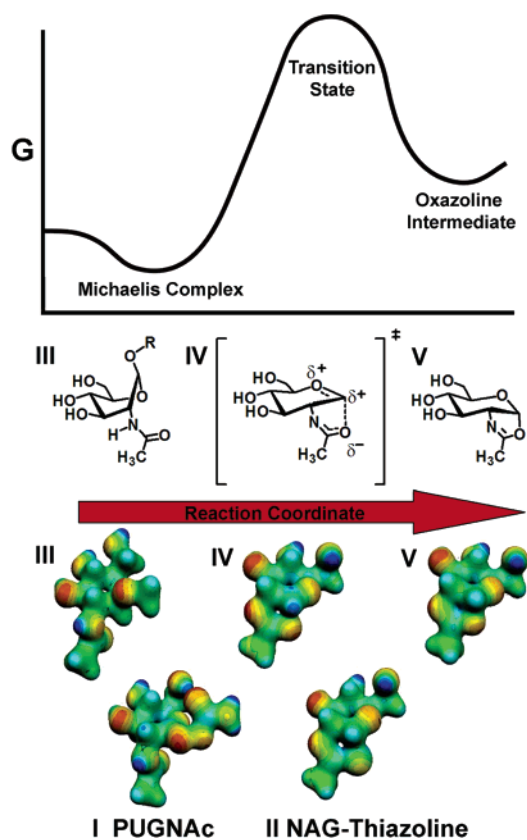


**Figure 6.** Simplified reaction coordinate for human *O*-GlcNAcase-catalyzed  $\beta$ -glucosaminide hydrolysis showing the MEPs for PUGNAc-analogue **I** (modeled with methyl rather than phenyl) and NAG-thiazoline **II** as well as ground state **III**, transition state model **IV**, and oxazoline **V**. NAG-thiazoline **II** is shown to share structural and electrostatic properties of both transition state model **V** and oxazoline **IV**. PUGNAc-analogue **I** is shown to share significant electrostatic properties with ground state **III**, although it does display some transition state-like conformational properties. MEPs (which all share a common scale) are shown projected onto the 0.04 electrons/ $\text{\AA}^3$  isodensity surface. Stick models of the calculated structures used to generate the MEPs are provided in the Supporting Information.

reasonable qualitative, though not quantitatively accurate, description of the reaction coordinate.

A comparison of our transition state model **IV** and the oxazoline **V** demonstrates that C–O bond extension is associated with both increased planarity about the anomeric carbon center as well as a contraction of the endocyclic C-1–O-5 bond. The most striking difference between oxazoline **V** and transition state model **IV**, however, is the build-up of positive charge, not only at the anomeric carbon center but also on the anomeric proton. This redistribution of charge is much more apparent than other changes centered about, for example, the endocyclic ring oxygen or within the oxazoline ring.

To afford a careful evaluation of this difference, we verified that this change in the MEP at the anomeric center was independent of the protonation state of oxazoline **V** by calculating similar MEPs for the associated oxazolinium ion, thiazo-

(60) Bagdassarian, C. K.; Schramm, V. L.; Schwartz, S. D. *J. Am. Chem. Soc.* **1996**, *118*, 8825–8836.

(61) Using a different distance constraint for the model involving the distance from the anomeric center to the 2'-carbon of the thiazoline ring leads to an even tighter TS model with respect to the distance between the anomeric center and the nucleophilic oxygen atom. This constraint allows the bond between the 2'-carbon and the nucleophilic oxygen bond to flex with the result that within the model it adopts a length greater than that found within the model of the oxazoline intermediate; a result that is inconsistent with the bond having an order between 1 and 2.



linium ion, and oxazolinium ion-based transition state model (in which the anomeric C–O bond length of the oxazolinium ion was constrained to that found in the thiazolinium ion). These MEPs may be found in the Supporting Information. A comparison of MEPs for the oxazolinium ion and the oxazolinium ion-based transition state model showed similarly significant changes in charge distribution on the anomeric carbon and hydrogen atoms (with an increase in positive character in the transition state model).

An analysis of the structure and MEP of thiazoline **II** reveals that it mimics some aspects of oxazoline **V** while in other aspects it more closely resembles the transition state model **IV**. The hexopyranose ring conformations of oxazoline **V**, thiazoline **II**, and transition state model **IV** are all subtly different. The model used for the reactivity of many glycosidases is one in which electrophilic migration of the anomeric carbon center enforces a conformational itinerary following the  ${}^1S_3$ – ${}^4H_3$ – ${}^4C_1$  path from Michaelis complex to enzyme-bound intermediate (Figure 6A). A comparison of our optimized structures indicates that, whereas the pyranose ring of transition state model **IV** is best described as a  ${}^4H_3$  conformation and that of NAG-thiazoline as adopting a  ${}^4C_1$  conformation, oxazoline **V** is best described as adopting a  ${}^4H_5$  conformation. This conformation is a result of C-3–C-2–C-1–O-5 coplanarity favored by formation of the five-membered oxazoline ring which induces strain in the pyranose ring. Although the precise conformational itinerary traveled along the reaction coordinate is uncertain, it seems likely that the less strained  ${}^4C_1$  conformation of thiazoline **II** lies conformationally closer to our transition state model.

Although NAG-thiazoline **II** bears a significant geometric resemblance to transition state model **IV**, a comparison of the MEPs for the three species under consideration reveal some subtle differences. The larger van der Waals radius of sulfur compared to oxygen is readily apparent when the MEPs are visualized. The potential surrounding the sulfur atom is also appreciably less negative than that surrounding the oxygen atom of either oxazoline **V** or transition state model **IV**. Furthermore, the potential distribution around the anomeric carbon and hydrogen atoms of thiazoline **II** most closely resembles that of oxazoline **V** when compared to that of transition state model **IV**.

The structural properties of thiazoline **II** and its MEP indicate that it is likely to be a reasonable mimic of a species that lies on the reaction coordinate between the region of the enzymic transition state and the enzyme-bound intermediate. PUGNac-analogue **I**, in contrast, displays a number of markedly different structural and electrostatic characteristics from oxazoline **V** and the transition state model **IV**. The hexopyranose ring of PUGNac-analogue **I** adopts a  ${}^4E$  conformation and, as such, is a marginally good mimic of the conformation of transition state model **IV**. In a number of critical respects, however, PUGNac-analogue **I** is an unsatisfactory mimic of either the oxazoline **V** or its preceding transition state. PUGNac-analogue **I** fails to capture any significant bonding between the *N*-acetamido moiety and the anomeric carbon center: as indicated previously, this interaction is a critical component of the reaction pathway at the transition state.<sup>30</sup> More critically, the MEP of PUGNac-analogue **I** indicates that there is significantly more negative potential in the region of the anomeric carbon atom. This negative potential is in striking contrast with the more positive

potential observed in oxazoline **V**, thiazoline **II**, and the transition state analogue **IV**. In this respect PUGNac-analogue **I** is significantly more substrate-like (structure **III**). The marked changes in charge at this center along the reaction coordinate are likely to be a significant target for *selective* transition state stabilization by human *O*-GlcNAcase, so any failure to mimic transition state charge at this center is likely to hinder the ability of PUGNac and derivatives to act as transition state analogues.

Another notable difference between NAG-thiazoline and PUGNac is that the polarizing residue (Asp<sup>174</sup> in human *O*-GlcNAcase<sup>30</sup> and Asp<sup>242</sup> in the *B. thetaiotaomicron*  $\beta$ -glucosaminidase<sup>57</sup>) is likely to engage in a much stronger interaction with oxazoline **IV** and thiazoline **II** as compared to PUGNac-analogue **I**. As noted previously,<sup>30</sup> the  $pK_a$  of the nitrogen atom will change during the cyclization step from around 15, for an amide proton, to a  $pK_a$  of about 5.5, the value found for the 2-methyl- $\Delta^2$ -oxazolinium ion.<sup>62</sup> The pH-rate profile ( $\log(K_M/k_{cat})$  vs pH) for the hydrolysis of *p*-nitrophenyl  $\beta$ -*N*-acetylglucosaminide allows us to assign a macroscopic  $pK_a$  value of approximately 5.0 to Asp<sup>174</sup>.<sup>30</sup> The  $pK_a$  of Asp<sup>174</sup>, therefore, much more closely matches those of the conjugate acids of thiazoline **II** and oxazoline **IV** than that of PUGNac-analogue **I**. Because hydrogen bonds between residues with closely matched  $pK_a$  values are stronger than those between residues whose  $pK_a$  values differ greatly, we may reasonably expect thiazoline-derived inhibitors to more tightly bind to Asp<sup>174</sup> than PUGNac-derived inhibitors. From the perspective of Asp<sup>174</sup>-binding, thiazoline-derived analogues will therefore be better transition state analogues than PUGNac-derived inhibitors, which possess greater ground state character in this particular interaction.

## Conclusion

Using three approaches, including linear free energy correlations, X-ray crystallographic analyses, and computational modeling, we find that NAG-thiazoline is a TS analogue for the human *O*-GlcNAcase catalyzed hydrolysis of  $\beta$ -glucosaminides while PUGNac is either a poor TS analogue or a serendipitous binding inhibitor. These observations are surprising in view of the conventional approaches used in the design of TS analogues of glycoside hydrolases. Specifically, PUGNac, which incorporates a traditional transition state design feature, an  $sp^2$ -hybridized anomeric center, is a poor TS mimic. NAG-thiazoline, which has an  $sp^3$ -hybridized anomeric center, is a good TS analogue even though such a geometry is not considered TS-like. It may appear counterintuitive that NAG-thiazoline, given the tetrahedral geometry of its anomeric center, should resemble the transition state for the hydrolysis of an acetal since these transition states are widely perceived as dissociative with significant oxocarbenium ion-like character. It seems more obvious that NAG-thiazoline may resemble the oxazoline structure found further along the reaction coordinate and be more of a mimic of a high-energy oxazoline intermediate. However, the C–S bond length of the thiazoline (1.86 Å) is considerably longer than the C–O bond length (1.45 Å) expected for the corresponding oxazoline. This longer bond

(62) Porter, G. R.; Rydon, H. N.; Schofield, J. A. *Nature* **1958**, *182*, 927.

(63) Kraulis, P. J. *J. Appl. Crystallogr.* **1991**, *24*, 946–950.

(64) Esnouf, R. M. *J. Mol. Graphics Modell.* **1997**, *15*, 132–134.

distance results in distortion of the pyranose ring of the thiazoline and mimics a bond order of 0.26 between the nucleophilic carbonyl oxygen and the anomeric center; a bond order consistent with the significant nucleophilic participation established previously.<sup>9</sup> Crystallographic studies, computationally determined structures, and molecular electrostatic potential surfaces for NAG-thiazoline- and PUGNAc-based inhibitors of human *O*-GlcNAcase support this view. On the basis of these qualitative MEPs, thiazoline-derived *O*-GlcNAcase inhibitors and related structures appear to be a better framework for capturing a substantial fraction of the transition state binding energy used by the enzyme when compared to PUGNAc-derived inhibitors. These collective results, in combination with earlier kinetics studies, also suggest late transition state poise for this electrophilic migration mechanism with significant nucleophilic participation and essentially no involvement of the leaving group—an observation consistent with studies of some of the N-ribosyl hydrolases. This improved understanding of the reaction coordinate adopted by human *O*-GlcNAcase, however qualitative, should provide the basis for the development and refinement of transition state analogues of human *O*-GlcNAcase having optimized geometries.

**Acknowledgment.** We thank the Western Canada research grid (WestGrid) for a generous allocation of resources. D.J.V. thanks the Natural Sciences and Engineering Research Council of Canada (NSERC) for support of this research. D.J.V. is a Michael Smith Foundation for Health Research (MSFHR) Scholar and is supported as a Tier II Canada Research Chair in Chemical Glycobiology. M.S.M. is supported as a Canada Graduate Scholar (NSERC) and by a graduate student fellowship from the MSFHR. G.J.D. thanks the Biotechnology and Biological Sciences Research Council and the Royal Society for funding. I.R.G. thanks the Royal Society (U.K.) for a postdoctoral fellowship to Canada.

**Supporting Information Available:** All experimental details, including those for the synthesis of compounds **3a–g** and **4a–g** as well as their structural proofs, enzyme assays, crystallographic studies, and computational studies; optimized geometries for all species described in the paper and MEPs for the protonated oxazolinium, thiazolinium, and oxazolinium-based transition state analogue; complete refs 4 and 5. This material is available free of charge via the Internet at <http://pubs.ac.org>.